

Structural Fluctuation and Concerted Motions in F₁-ATPase: A Molecular Dynamics Study

YUKO ITO, MITSUNORI IKEGUCHI

Graduate School of Nanobioscience, Yokohama City University, 1-7-29, Suehiro-cho,
Tsurumi-ku, Yokohama 230-0045, Japan

Received 28 October 2009; Revised 17 December 2009; Accepted 25 December 2009

DOI 10.1002/jcc.21508

Published online 24 March 2010 in Wiley InterScience (www.interscience.wiley.com).

Abstract: F₁-ATPase is an adenosine tri-phosphate (ATP)-driven rotary motor enzyme. We investigated the structural fluctuations and concerted motions of subunits in F₁-ATPase using molecular dynamics (MD) simulations. An MD simulation for the $\alpha_3\beta_3\gamma$ complex was carried out for 30 ns. Although large fluctuations of the N-terminal domain observed in simulations of the isolated β_E subunit were suppressed in the complex simulation, the magnitude of fluctuations in the C-terminal domain was clearly different among the three β subunits (β_E , β_{TP} , and β_{DP}). Despite fairly similar conformations of the β_{TP} and β_{DP} subunits, the β_{DP} subunit exhibits smaller fluctuations in the C-terminal domain than the β_{TP} subunit due to their dissimilar interface configurations. Compared with the β_{TP} subunit, the β_{DP} subunit stably interacts with both the adjacent α_{DP} and α_E subunits. This sandwiched configuration in the β_{DP} subunit leads to strongly correlated motions between the β_{DP} and adjacent α subunits. The β_{DP} subunit exhibits an extensive network of highly correlated motions with bound ATP and the γ subunit, as well as with the adjacent α subunits, suggesting that the structural changes occurring in the catalytically active β_{DP} subunit can effectively induce movements of the γ subunit.

© 2010 Wiley Periodicals, Inc. J Comput Chem 31: 2175–2185, 2010

Key words: F₁-ATPase; molecular dynamics; structural dynamics; correlation matrix; contact analysis

Introduction

F₀F₁-ATPase synthase produces adenosine tri-phosphate (ATP) coupled with proton transport across membranes, driven by the electrochemical diffusion gradient.^{1–12} The water-soluble, F₁ part of ATP synthase comprising five subunits (α – ϵ) is known as a rotary molecular motor (Fig. 1A). X-ray crystallography of F₁-ATPase in 1994 elucidated that the $\alpha_3\beta_3$, nucleotide-binding subunits are arranged hexagonally around the γ subunit.¹³ The α and β subunits consist of three domains: the N-terminal, nucleotide-binding, and C-terminal domains. ATP is bound in the nucleotide-binding domain. The actual ATP binding site resides in the interface between the α and β subunits, and the substrate binding residues are drawn from each subunit. Only ATP bound in the β subunits is catalytically active, resulting in three actual active sites for the catalytic reaction. Although crystal structures have been solved under different conditions since the first in 1994,¹³ the β subunit tends to adopt the three different conformations: two closed (β_{DP} and β_{TP}) states and one open (β_E) state. Only one crystal structure, determined in 2001, has a half-closed β subunit (β_{HC}) instead of the open one (β_E),¹⁴ and this appears to represent a different reaction state.

The rotation of the central γ subunit has been proven using single molecule fluorescent microscopy.^{15,16} The hydrolysis

reaction of F₁-ATPase, accompanying the structural conversion of the β subunit, occurs in the 120° rotation step of the γ subunit,¹⁷ which can be divided further into 80° and 40° substeps. It has been found that ATP binds to an active site before the first partial 80° rotation of the γ subunit. Subsequent ATP hydrolysis occurs for 1 ms, followed by the 40° rotation.^{18,19} At the catalytic dwell state (before the 40° rotation), the rotation of the γ subunit is occasionally inhibited by ADP.²⁰ As most of crystal structures essentially represent the same state, several hypotheses concerning which reaction states correspond to the crystal structures have been proposed.^{21–25} Eventually, single molecule studies using disulfide crosslinking proved that these crystal

Additional Supporting Information may be found in the online version of this article.

Correspondence to: M. Ikeguchi; e-mail: ike@tsurumi.yokohama-cu.ac.jp
Contract/grant sponsors: Ministry of Education, Culture, Sports, Science, and Technology (MEXT; Grants-in-Aid for Scientific Research); Japan Science and Technology Agency; Research and Development of the Next-Generation Integrated Simulation of Living Matter (a part of the Development and Use of the Next-Generation Supercomputer Project of MEXT)

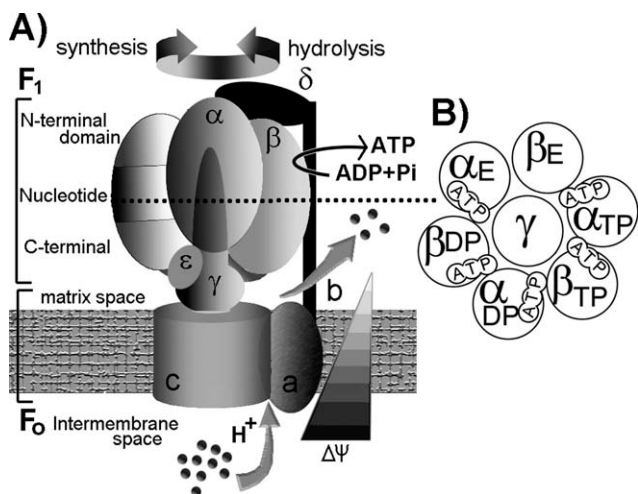


Figure 1. (A) Structure of F₁F₀-ATP synthase, and (B) the cross-sectional arrangement of the subunits in the F₁ moiety, viewed from the side of the C-terminal domains.

structures represented the catalytic dwell state.^{26,27} Another single-molecule experiment study showed that during the 40° rotation, the β_{DP} subunit undergoes structural changes from the closed to partially closed conformation, while the other β_E and β_{TP} subunits retain the same conformations, as in the catalytic dwell state.²⁸

Recently, another single molecule experiment has revealed that even when most of the axle of the γ subunit is removed, it still retains its rotation in the correct direction, as well as its ATP hydrolysis activity.^{29,30} This result suggests that the sequential structural transitions of the three β subunits take place even without most of the axle of the γ subunit, and thus cooperative motions of the α and β subunits are crucial for the γ subunit rotation.

As F₁-ATPase has unique properties of both structure and function, many computer simulations have been applied to this protein.^{21,22,31–40} Quantum mechanics and molecular mechanics (QM/MM) simulations have predicted the chemical reaction pathway for ATP hydrolysis.^{31,32} Targeted and biased molecular dynamics (MD) simulations have calculated the structural transition for the γ subunit 120° rotation,^{33,34} and coarse-grained MD simulations have determined the substep structures for the 80° and 40° rotations.^{21,22}

Equilibrium structural fluctuations of proteins have been theoretically and experimentally proven to be related to functionally important conformational changes.^{41–43} From this perspective, normal mode analysis has been applied to F₁-ATPase for investigation of the relationship between structural fluctuations and conformational changes.^{36,38,39} Linear response theory has shown that equilibrium fluctuations of proteins link perturbations (e.g., ligand binding and chemical reactions) with their responses (i.e., protein conformational changes).⁴⁰

The asymmetrical nature in the quasi-three fold symmetrical structure of the F₁-ATPase complex is closely related to the γ subunit rotation. The most prominent asymmetrical feature in the F₁-ATPase structure is the β subunit conformations, that is,

one open and two closed conformations. Moreover, the two closed β subunits are functionally different. For example, only the β_{DP} subunit has the ability of ATP hydrolysis. Therefore, it is of great interest to get an insight into the asymmetrical nature in the F₁-ATPase complex, in particular, from the perspective of structural dynamics and fluctuations. Here, we performed all-atom MD simulations for the F₁-ATPase α₃β₃γ complex and explore the asymmetrical properties using analysis of the structural fluctuations. From this analysis, we found asymmetry in subunit fluctuations, arising from different interface configurations between subunits in the hexamer ring. The different interface configurations also affect the concerted motions of subunits. The analysis highlights an extensive network of highly correlated movements of the β_{DP} subunit with the neighboring α and γ subunits and bound ATP. The inherent asymmetrical dynamics of the F₁-ATPase complex provide important clues toward understanding the rotation mechanism of the γ subunit.

Materials and Methods

The initial structure of the α₃β₃γ complex was taken from the crystal structure (PDB ID: 2JDI),⁴¹ the missing residues of which (α_{TP}402–409, β_E388–395, γ48–66, 87–104, 117–126, 149–158, and 174–205) were added using MODELLER,⁴² based on the crystal structure (PDB ID: 1E79),⁴³ and were optimized by energy minimization. AMP-PNP molecules in the β_{DP} and β_{TP} subunits of the original crystal structure (PDB ID: 2JDI) were replaced by ATP, since the complex structure is assumed to be in the catalytic dwell state.²⁶ The total number of atoms is 337,300. All simulations were carried out with the MD program MARBLE,⁴⁴ using CHARMM22/CMAP^{45,46} for protein and TIP3P⁴⁷ for water, as force field parameters. Electrostatic calculations were performed using the particle mesh Ewald method with periodic boundary conditions.⁴⁸ The Lennard-Jones potential is truncated at 10 Å. In this study, the symplectic integrator for rigid bodies was used for constraints of the bond lengths and angles involving hydrogen atoms.⁴⁴ The time step used was 2.0 fs.

The whole system was equilibrated for 100 ps, constraining the protein coordinates under the NPT ensemble (300 K and 1 atm) condition, with a harmonic force constant of 1 kcal/mol/Å². Subsequently, the force constant gradually decreased to zero over 100 ps. Sampling MD simulations were performed under the NPT ensemble conditions for 30 ns.

Results

β_E Subunit Fluctuation in the F₁-ATPase Complex

The changing dynamics of the isolated β subunits for formation of the complex are shown in Figure 2A; a comparison of the residue-based root mean square fluctuation (RMSF) between the isolated (TF₁ and MF₁) and complex open (β_E) subunits. The former data was derived from our different study. The RMSF was calculated via a superposition of the trajectory conformations and the reference conformation (i.e., the average structure). The RMSF is defined as

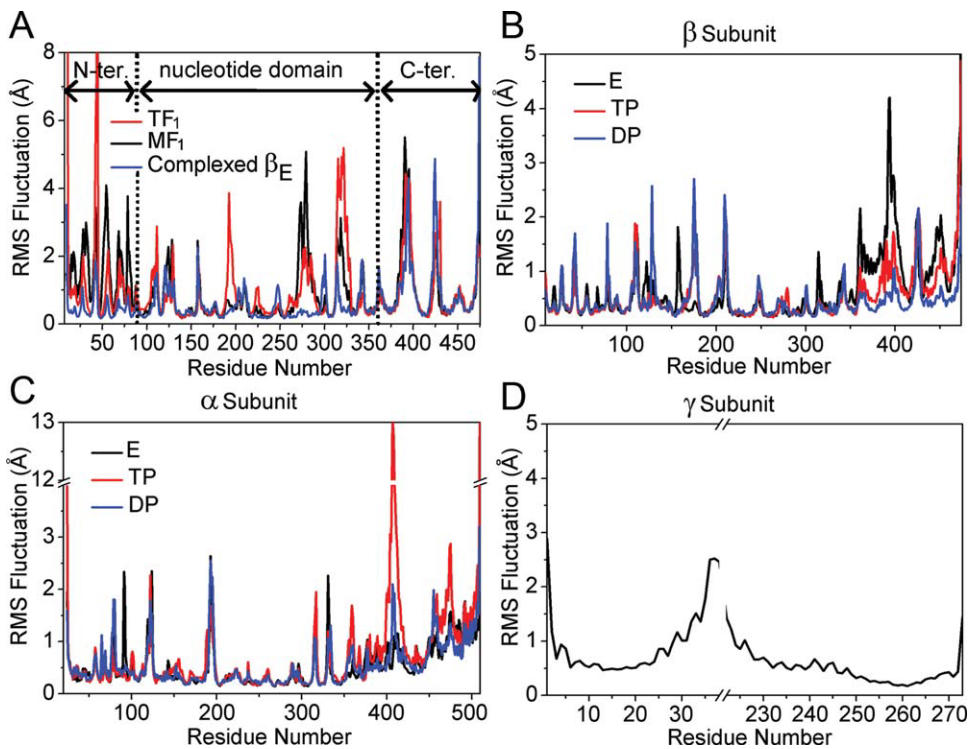


Figure 2. (A) RMSF versus residue number for isolated TF₁ (red), MF₁, (black) and the complexed β_E (blue). RMSF for the (B) β subunits, (C) α subunits, and (D) γ subunit. This RMSF calculation of the F₁-ATPase complex was performed without the protruding region of the γ subunit.

$\text{RMSF}(i) = \sqrt{\langle (\mathbf{R}_i - \langle \mathbf{R}_i \rangle)^2 \rangle}$, where \mathbf{R}_i is the position vector of atom i (in this study, only the C_α atom coordinates were evaluated) and the chevron brackets represent the time average over the whole trajectory. The RMSF indicates the structural flexibility for each residue.

The large fluctuations observed in the isolated β_E subunits were significantly suppressed at the N-terminal and nucleotide-binding domains of the complexed β_E subunit (Fig. 2A). In particular, the fluctuation of the entire N-terminal domain is strongly suppressed. In the nucleotide-binding domain, suppression of the fluctuation appears in three regions: β_ETyr180–Met200 (sheet-4 and helix-c), and loops β_EGly273–Gly280 and β_EAsp315–Asp319, since these regions are located at the interface with the other subunits. The β_ETyr180–Met200 region interacts with the α subunit (α_EAla133–Val142), while the β_EGly273–Gly280 and β_EAsp315–Asp319 loops interact with the γ subunit.

Interestingly, the fluctuation of the C-terminal domain is not suppressed at all. As described later, this is closely related to interface configurations with adjacent subunits.

Each Subunit Fluctuation

The RMSF for the β, α, and γ subunits is shown in Figures 2B–2D, respectively. A schematic representation of the cross-sectional location of the subunits in F₁-ATPase is shown in Figure 1B. Under physiological conditions, a portion of the γ subunit protruding from the α₃β₃γ complex is attached to the ε subunit

and is embedded in the c subunit oligomeric ring (see Fig. 1A). As this simulation does not include the ε subunit or the c subunit ring, the γ subunit protrusion is considerably flexible (Supporting Information Fig. S1). Because we focus here on the fluctuation of the α and β subunits and the axle of the γ subunit, the γ subunit protrusion (γLys39-Thr221) was omitted from RMSF calculations in this study.

β Subunits

The magnitude of the fluctuations of the whole C-terminal domain is clearly different between the three states of the β subunit (Fig. 2B). The β_E, β_{TP}, and β_{DP} subunits show the largest, intermediate, and smallest fluctuations at the C-terminal domain, respectively. The difference in the fluctuations between the β_{TP} and β_{DP} subunits is particularly interesting, because both subunits bind the same nucleotide, that is, ATP in this simulation, and the structures of the β_{TP} and β_{DP} subunits are almost identical (the C_α -RMSD between β_{TP} and β_{DP} in 2JDI is 0.67 Å). This difference in the fluctuation of the C-terminal domain appears to be derived from differences in the interface configurations between the β_{TP} and β_{DP} subunits (described later).

α Subunits

The large movement in the C-terminal domain of the α_{TP} subunit is also the most outstanding difference among the three α subunits (Fig. 2C). This movement is ascribed to the interface arrangement of the α subunits in the F₁-ATPase complex. Apart

from this large movement of the α_{TP} subunit, fluctuations are almost the same over all the α subunits, in magnitude and localization (described later).

γ Subunit

Because the flexible parts are omitted from the RMSF calculation, no remarkable fluctuations are detected in the two coils of the γ subunit (Fig. 2D). Once the γ subunit becomes a part of complex, this portion appears to be relatively stable.

Correlation Matrix

For further investigation, the degree of correlated fluctuations between intrasubunit residues was analyzed using the correlation matrix technique.⁴⁹

The magnitude of correlated motions between residues is given by $C_{ij} = \frac{\langle (\mathbf{R}_i - \langle \mathbf{R}_i \rangle) \cdot (\mathbf{R}_j - \langle \mathbf{R}_j \rangle) \rangle}{\sqrt{\langle (\mathbf{R}_i - \langle \mathbf{R}_i \rangle)^2 \rangle \cdot \langle (\mathbf{R}_j - \langle \mathbf{R}_j \rangle)^2 \rangle}}$, where \mathbf{R}_i is the position vector of each pair of C_x atoms, i and j , and the chevron brackets represent the ensemble average. The matrix element C_{ij} is distributed in the range of -1 to 1 ; the correlation is 1 for completely synchronized oscillation of the two atoms (i.e., moving in the same direction with same periodicity), or -1 for anti-synchronization. If each motion is independent, or fluctuates in orthogonal directions, then the correlation is 0 . In the correlation matrix, red represents strong positive correlation and dark blue represents negative correlation.

The map patterns of the correlation matrices are fairly similar for all α and β subunits (see Fig. 3). Surprisingly, even α subunits believed to lack a dynamic conformational change during γ rotation display a similar map pattern to that of the β subunits. The main similarities between the β and α subunits in the correlation matrix include: (1) strongly correlated motions within each of the N-terminal, nucleotide-binding, and C-terminal domains; (2) weak correlation between motions of the N-terminal and C-terminal domains; and (3) strong correlation among motions of the C-terminal domain and those of three separated regions in the nucleotide-binding domain: a part of helix A (β Gln130-Lys148 and α Gln147-Val157), the region including the P-loop motif (β Gly159-Ala174 and α Leu166-Arg188), and the region including adenine-binding residues (β Thr332-Thr354 and α Gly348-Arg373).

The correlation matrix of the β_{DP} subunit is slightly different from the other subunits. A slight positive correlation (green color) is spread more extensively than in other subunits; particularly the two areas exhibiting correlated motions between the N-terminal and nucleotide-binding domains, and between the nucleotide-binding and C-terminal domains. Together with the small RMSF of the C-terminal domain in the β_{DP} subunit (Fig. 2B), this suggests that the β_{DP} subunit oscillates more as a rigid body than as a hinge-bending motion, which appears to relate to the unique interface arrangements of the β_{DP} subunit (described later).

α/β Subunit Interface

The interface interactions of the catalytic pairs ($\alpha_E\beta_E$, $\alpha_{TP}\beta_{TP}$, and $\alpha_{DP}\beta_{DP}$) and the noncatalytic pairs ($\beta_E\alpha_{TP}$, $\beta_{TP}\alpha_{DP}$, and $\beta_{DP}\alpha_E$) were investigated using the intersubunit correlation matrix and stable contacts analysis, (Figs. 4 and 5, respectively).

In the analysis of stable contacts,⁵⁰ intersubunit residue pairs maintaining their interatomic distances at less than 4.5 \AA for 98% of snapshots in the MD trajectory were detected. All residues detected by this method are listed in the Supporting Information Table S1.

C-Terminal Domain (α Thr380-Ala510/ β Gly364-Ala474)

In the contact analysis, the interface of the C-terminal domain shows remarkable differences over all the catalytic and noncatalytic pairs. Stable contacts in the C-terminal domain are observed only in the β_{DP} subunit, that is, interfaces $\alpha_{DP}\beta_{DP}$ and $\beta_{DP}\alpha_E$ (Fig. 5; yellow line). Correspondingly, strongly correlated motions of the C-terminal domains are also observed only in the $\alpha_{DP}\beta_{DP}$ and $\beta_{DP}\alpha_E$ subunit pairs (see Fig. 4). Residues corresponding to these strong correlation points are listed in Supporting Information Table S2. Regarding ATP binding in the β_{DP} subunit, residues (β Ala340-Gly343 and β Arg408-Ser415) lying next to the adenine-binding regions make stable contacts and move concerted with the α_{DP} subunit. The stable interaction of the C-terminal domains in the $\alpha_{DP}\beta_{DP}$ subunit pair appears to affect the fluctuation of the ATP molecule (described later).

Among the six α and β subunits, only the β_{DP} subunit has a tight sandwiched configuration. In contrast to the tight interfaces of the β_{DP} subunit, neither the $\alpha_{TP}\beta_{TP}$ nor $\beta_{TP}\alpha_{DP}$ subunit interface of the C-terminal domain is tightly packed. Strong correlations are not observed in the C-terminal domain of the $\alpha_{TP}\beta_{TP}$ or $\beta_{TP}\alpha_{DP}$ subunit pair either. Therefore, the small RMSF of the C-terminal domain in the β_{DP} subunit, compared to the β_{TP} subunit, seems to be derived from the tightly sandwiched β_{DP} interfaces (Fig. 2B). In addition, the tight β_{DP} interfaces also suppress the RMSF of the C-terminal domain in the α_E and α_{DP} subunits, because those α subunits make stable contacts with the β_{DP} subunit in the C-terminal domain (Figs. 2C and 5). By contrast, the RMSF of the C-terminal domain in the α_{TP} subunit is large, due to the lack of stable contacts with adjacent subunits. These interface configurations have also been observed in other crystal structures, such as 1BMF,¹³ 1E79,⁴⁷ 1W0J,⁵¹ and 1E1Q.⁵²

Nucleotide-Binding Domain (α Asp96-Gln379/ β Arg83-Val363)

Contact analysis shows that the nucleotide-binding domain has similar interfaces in all the catalytic and noncatalytic subunit pairs (Fig. 5; cyan lines). However, the correlation matrices of the nucleotide-binding domain are not as uniform, especially for the $\alpha_{DP}\beta_{DP}$ pair (Fig. 4 and Supporting Information Table S2).

In the catalytic subunit pair, the $\alpha_{DP}\beta_{DP}$ pair displays a different correlation map pattern from the $\alpha_E\beta_E$ and $\alpha_{TP}\beta_{TP}$ pairs. In the $\alpha_{DP}\beta_{DP}$ pair, motions of the ATP-binding residues in the nucleotide-binding domains are less correlated than in the $\alpha_E\beta_E$ and $\alpha_{TP}\beta_{TP}$ pairs (Fig. 4 and Supporting Information Table S2). Instead, the ATP-binding residues in the β_{DP} subunit move concerted with the C-terminal domains of α_{DP} and β_{DP} , which is not observed in other catalytic subunit pairs ($\alpha_E\beta_E$ and $\alpha_{TP}\beta_{TP}$). Apart from the $\alpha_{DP}\beta_{DP}$ pair, the loose packing at the $\alpha_E\beta_E$ interface (the number shown in Fig. 5) might facilitate ATP entering the catalytic cavity.

Conversely, all correlation matrices generally have a similar map pattern for the noncatalytic subunit pairs. As stable contacts

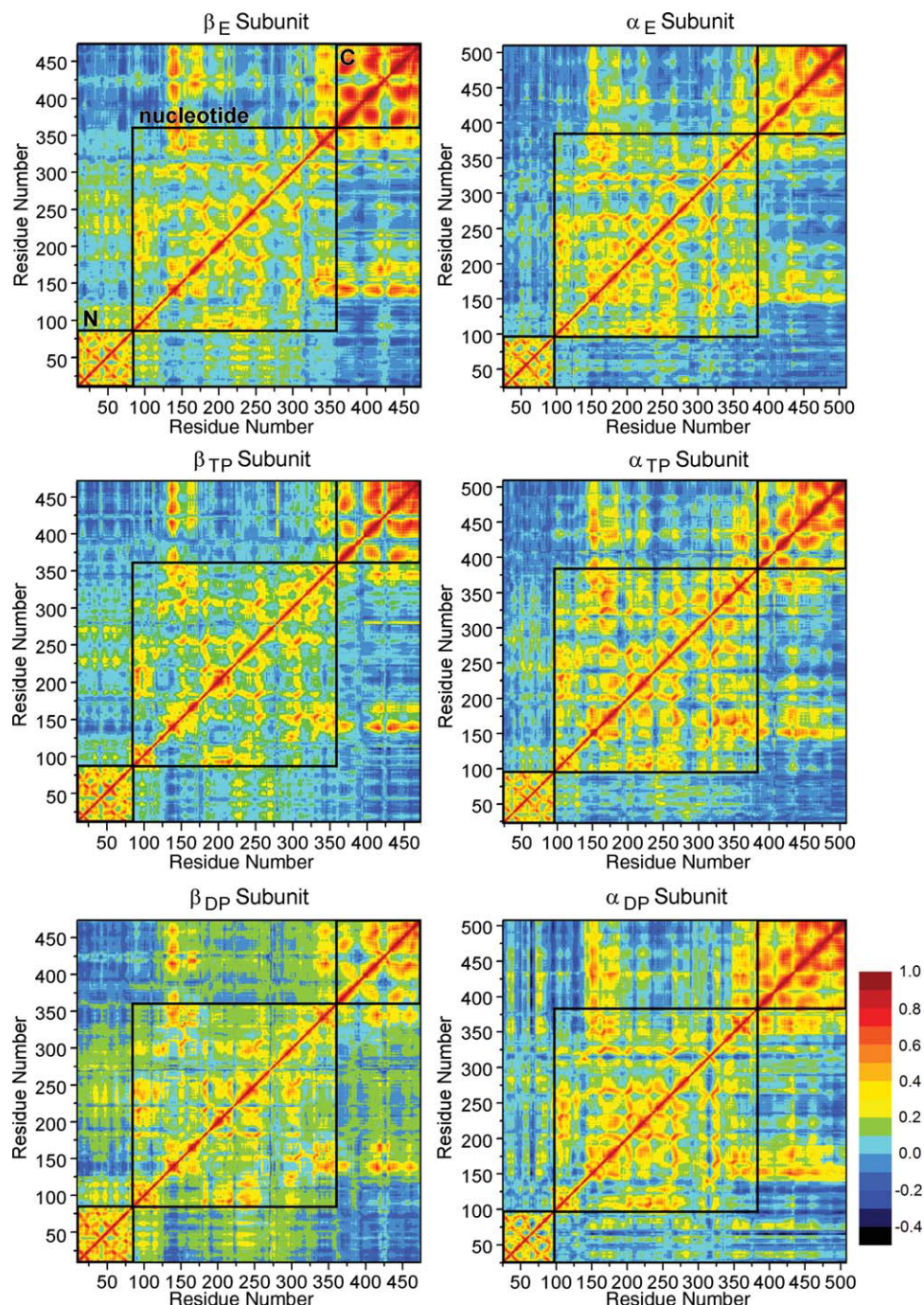


Figure 3. Intrasubunit correlation matrix for the β and α subunits. The N-terminal, nucleotide-binding, and C-terminal domains are present as black frames.

at the interface of the nucleotide-binding domain (yielded by contact analysis) are formed by identical residue combinations in all noncatalytic subunit pairs, strong positive correlation appears at the same position in all the correlation matrices. However, motions of the $\beta_E\alpha_{TP}$ pair have weak correlation relative to those of the $\beta_{TP}\alpha_{DP}$ and $\beta_{DP}\alpha_E$ pairs. These weakly correlated motions of the nucleotide-binding domains in the $\beta_E\alpha_{TP}$

pair are probably affected by strong oscillations of the C-terminal domain of both α_{TP} and β_E , as observed in the RMSF (Figs. 2B and 2C). Moreover, contact analysis shows that the total number of stable contacts at the interface of this $\beta_E\alpha_{TP}$ pair is smaller than in the other noncatalytic subunits (see Fig. 5), thus suggesting a looser interface in the $\beta_E\alpha_{TP}$ pair than in the other noncatalytic pairs.

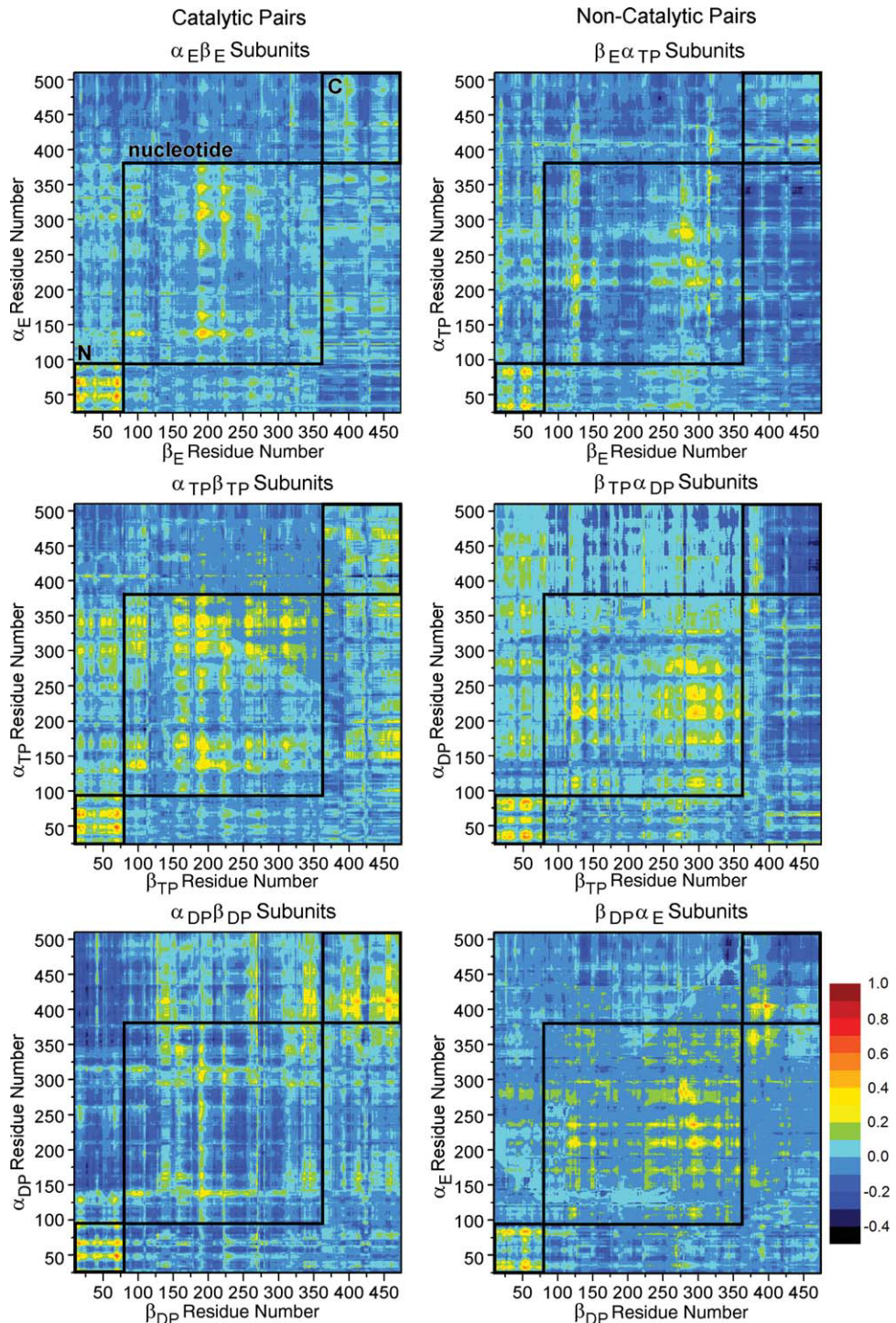


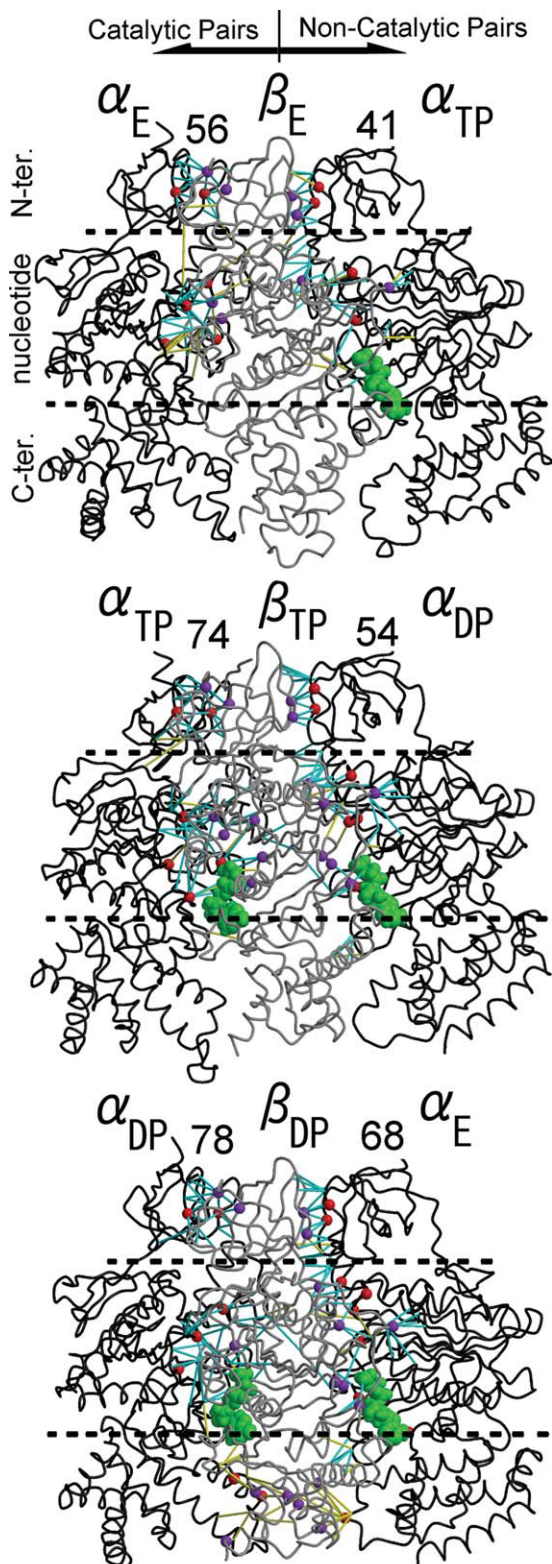
Figure 4. Intersubunit correlation matrix for the α and β subunits. The three domains (N-terminal, nucleotide-binding, and C-terminal domains) are enclosed by black frames.

N-Terminal Domain (α Asp24-Val95/ β Thr9-Ile82)

In contact analysis, all the α and β subunit interfaces of the N-terminal domain have identical contacts (Fig. 5; cyan lines). Correspondingly, in the correlation matrix, similar map pat-

terns (i.e., four strongly correlated sites between the intersubunit residues; yellow and red spots in Fig. 4), are observed for all the catalytic/noncatalytic pairs (Supporting Information Table S2). The four points of the matrix in all catalytic and noncatalytic pairs occur at the same residue intersections,

which correspond to the center of the α and β subunit interface, as indicated by the red (α subunit) and purple (β subunit) spheres in Figure 5.



At these four points, the bulky residues (e.g., Leu, Ile, and Lys) tend to be assembled. Accordingly, the almost identical interfaces (observed in contact analysis, Fig. 5) and the strong correlation in the correlation matrices for the N-terminal domain can be ascribed to hydrophobic interactions with the bulky alkyl side-chains. Moreover, several Gly and Ala residues are also observed around the bulky residues (e.g., β Gly11, Ala15, Gly18, and Ala19), suggesting that these flexible residues play the role of elastic elements for continuously maintaining hydrophobic interactions during the structural change with the rotation of the γ subunit. The symmetrical interfaces, resulting in the doughnut-like rigid-body in the hexamer, imply that RMSF of the N-terminal domain in the complexed β_E are strongly suppressed (Fig. 2A). Consequently, the hydrophobic interactions at the four points seem to contribute strongly to the structural stability of the entire N-terminal domain.

$\beta\gamma$ Subunit Interface/ $\alpha\gamma$ Subunit Interface

To probe the structural relation between the β/α subunits and the γ subunit, correlation matrices and contact analysis are applied to these pairs (Figs. 6, 7, and Supporting Information Table S3). In the F_1 -ATPase complex, the portion of the β and α subunits that interact with the γ subunit are limited to the residues β Gly273–Gly280, β Asp315–Asp319, α Arg286–Ala293, and α Ala331–Ser335, corresponding to the loops facing towards the γ subunit in the nucleotide binding domain, and the helix-turn-helix (HTH) motif of the C-terminal domain of the β and α subunits (see Fig. 7).

$\beta\gamma$ Subunit Interface

All the β subunits contact the γ subunit via the two loops in the nucleotide-binding domain and the HTH part of the C-terminal domain (see Fig. 7). The correlation matrix shows different characteristics for each β subunit. In the $\beta_E\gamma$ pair, mainly the loops of the nucleotide-binding domain of the β_E subunit have stable contacts (see Fig. 7). In contrast to the β_E subunit, in the β_{TP} and β_{DP} subunits, the HTH portion of the C-terminal domain, which is essential for γ rotation,^{35,36} has many stable contacts and moves concerted with the γ subunit. In particular, a broad area of the β_{DP} subunit undergoes relatively correlated motions with the γ subunit, as compared to the other subunits.

$\alpha\gamma$ Subunit Interface

Contact analysis reveals that either one or both of the two loops in the nucleotide-binding domain make stable contacts with the γ

Figure 5. Contact analysis results for the α and β subunits, showing interface contacts. Cyan indicates stable contacts formed by identical residue pairs across the catalytic or noncatalytic pairs, and yellow indicates stable contacts of a unique residue combination in the subunit interface. The ATP molecule is colored green. Red and purple spheres represent interface residues of the α and β subunits, respectively, undergoing strongly correlated motions detected using the correlation matrices. The numbers indicate the net number of stable contacts in the α and β subunit interface.

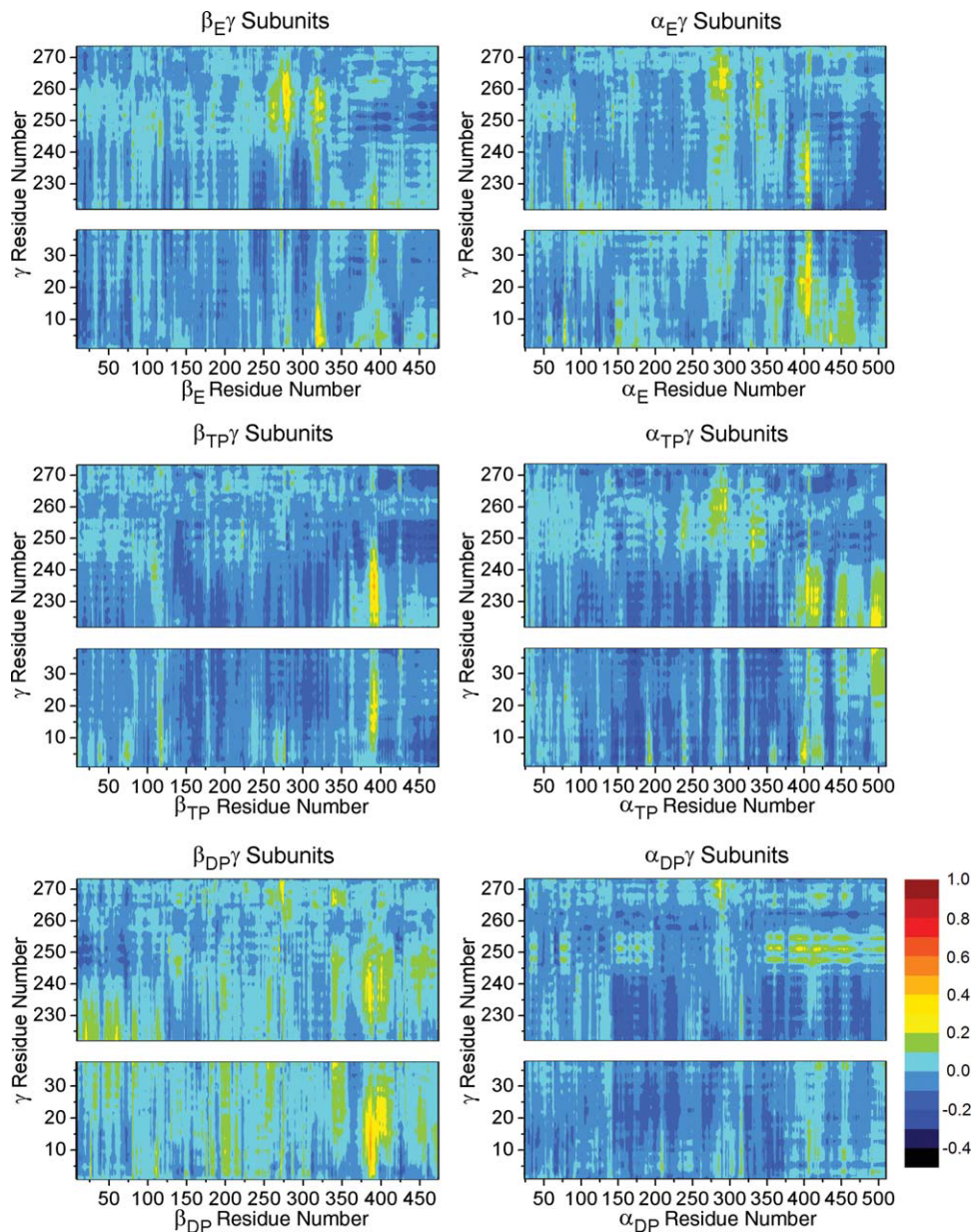


Figure 6. Intersubunit correlation matrix between the β/α subunits and the γ subunit. Depicted residues of the γ subunit are γ Ala1-Leu38 and γ Thr222-Asp273.

subunit in all the α subunits, and only the α_E subunit interacts with the γ subunit via the HTH part of the C-terminal domain (see Fig. 7). In addition to contact analysis, only the HTH portion of the α_E subunit exhibits strongly correlated motions with the γ subunit in the correlation matrix (see Fig. 6). Motions of the α_{TP} subunit have a particularly weak correlation. Consequently, even though the loops of the nucleotide-binding domain in the α_{TP} and α_{DP} domains reside close to the γ subunit, it may be that only the α_E subunit is related to movements of the γ subunit in this state.

β Subunit and ATP

Figure 8 shows the correlation matrices between motions of the $\beta_{DP/TP}$ subunit and bound ATP. It is found that ATP bound to the β_{DP} subunit moves in concert with the P-loop region (β Gly156–Thr163) and the adenine-binding region (β Ile344–Ala347 and β Phe418–Thr425). Surprisingly, motions of adenine-binding residues in the β_{DP} subunit are also correlated with the ribose and phosphate groups of ATP (Fig. 8B), even though those parts do not interact directly. In contrast to β_{DP} , the adenine-binding resi-

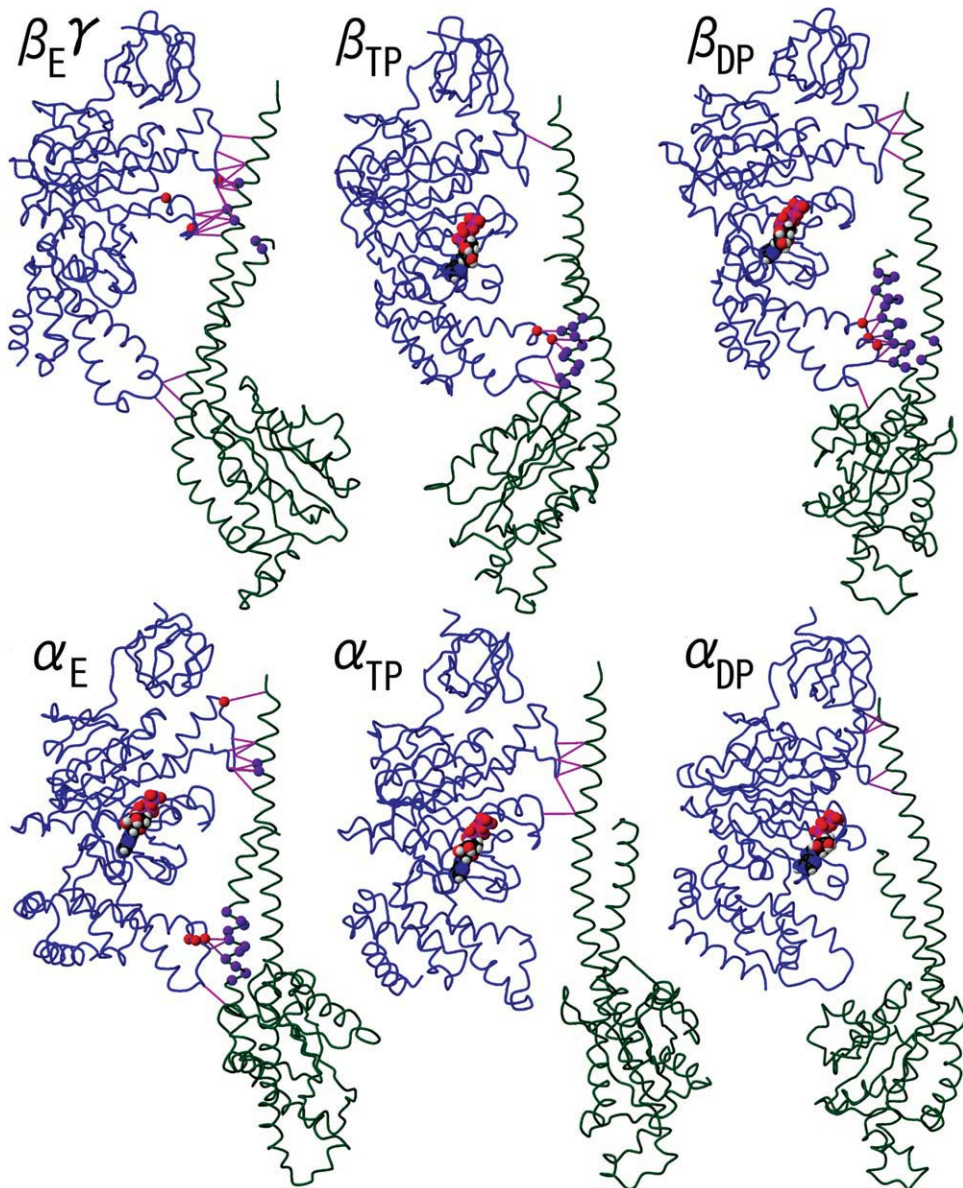


Figure 7. Stable contacts between the β/α subunits and the γ subunit, detected via contact analysis. Magenta lines indicate stable contacts during the MD simulation, and purple spheres indicate interface residues undergoing strongly correlated motions in the correlation matrices.

dues in the β_{TP} subunit exhibit relatively weak correlations with ATP (Fig. 8C).

Discussion

Once the complex is formed, the fluctuation of the N-terminal domain of the β_E subunit is suppressed dramatically and only the C-terminal domain fluctuates dynamically (Fig. 2A, blue line). Bulky and hydrophobic residues contribute to this suppression in the N-terminal domain of the β subunit, thereby maintaining stable contacts with adjacent α subunits.

In contrast, the magnitude of the fluctuations in the C-terminal domain is clearly different among the β_E , β_{TP} , and β_{DP} subunits (Fig. 2B). In particular, notwithstanding the fairly similar nucleotide-bound conformations of the β_{TP} and β_{DP} subunits, the fluctuation of the C-terminal domain in the β_{DP} subunit is significantly smaller than in the β_{TP} subunit (Fig. 2B), due to differences in their interface configurations. In addition to the tight packing configuration of the $\alpha_{DP}\beta_{DP}$ interface, the $\beta_{DP}\alpha_E$ subunit interface (on the opposite side of the β_{DP} interface), has additional stable contacts in the C-terminal domain. In contrast to these tight β_{DP} interfaces, the C-terminal domain of β_{TP} has no stable contacts with the adjacent two α subunits (see Fig. 5).

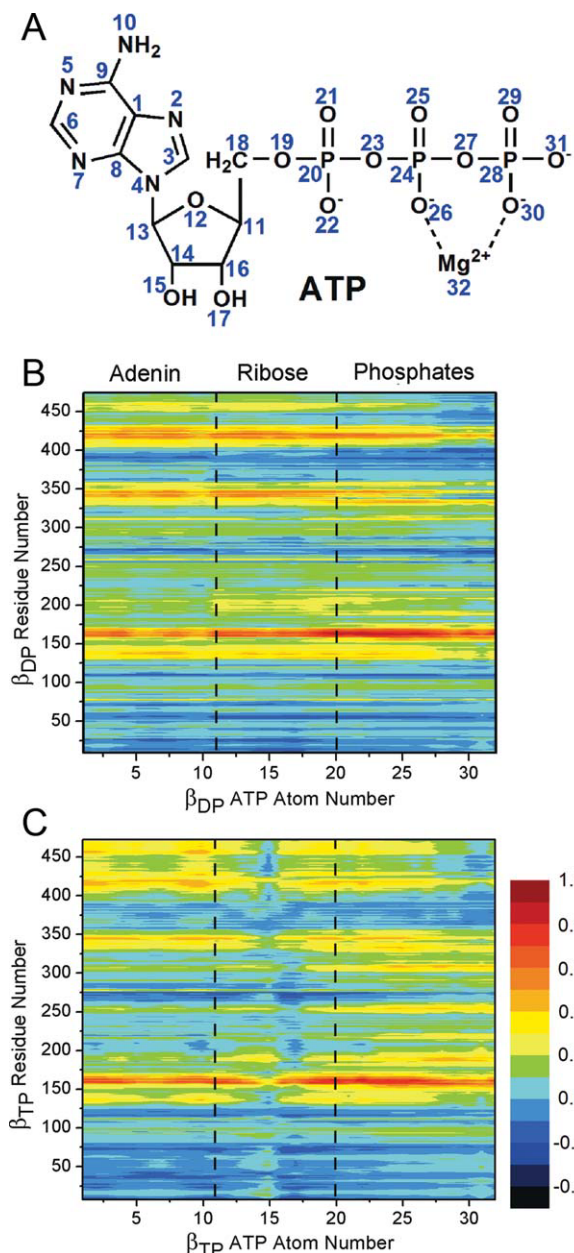


Figure 8. (A) ATP chemical structure in which nonhydrogen atoms are numbered. (B) The correlation matrix between the C_x atoms of the β_{DP} subunit and ATP bound in the β_{DP} subunit. (C) is the same as (B), but for the β_{TP} subunit.

These different interface configurations also influence concerted movements of the β_{DP} and β_{TP} subunits with adjacent subunits. The tightly packed C-terminal domain of the β_{DP} subunit moves in concert with the adjacent α_E and α_{DP} subunits (see Fig. 4). By contrast, in the β_{TP} subunit, motions of the C-terminal domain are only weakly correlated with residues of its adjacent α subunits. The difference between the β_{DP} and β_{TP} subunits is also observed in correlated motions involving ATP molecules bound to the subunits (see Fig. 8). The fluctuation of ATP and all its binding residues (the P-loop and adenine-binding regions) is

highly synchronized in the β_{DP} subunit. Conversely, only the residues around the P-loop have strong positive correlation in the β_{TP} subunit.

The concerted movements in the nucleotide and C-terminal domains are summarized in Figure 9. The C-terminal domain of the β_{DP} subunit has an extensive network of highly correlated motions with the bound ATP and adjacent subunits (α_{DP} , α_E , and γ ; Fig. 9, red lines). Within the β_{DP} subunit, motions of the P-loop and adenine-binding regions are highly correlated with the C-terminal domain (see Fig. 3). The fluctuations of those regions are also correlated strongly with those of the entire ATP molecule (Fig. 8B). Moreover, the residues lying next to the adenine-binding region exhibit strongly correlated motions with residues of the α_{DP} subunit (Fig. 4, Supporting Information Table S2) and a broad portion of the β_{DP} subunit moves in concert with the γ subunit (see Fig. 6).

Single-molecule experiments,^{26,27} as well as theoretical QM/MM^{31,32} and free-energy MD simulations,^{9,53} have identified that the ATP hydrolysis reaction occurs at the β_{DP} subunit in the catalytic-dwell state. According to the recent application of linear response theory to protein conformational changes, equilibrium fluctuations link perturbations (e.g., ligand binding and chemical reaction) with their responses (i.e., protein conformational changes).⁴⁰ Therefore, the highly correlated motions between ATP-binding residues and the C-terminal domain of the β_{DP} subunit may facilitate transmission of structural perturbations arising from ATP hydrolysis into the C-terminal domain of the β_{DP} subunit.

A single-molecule experiment study has shown that during the 40° rotation of the γ subunit after ATP hydrolysis and phosphate release,⁵⁴ the β_{DP} subunit undergoes structural changes from the closed to partially closed conformation, while the other

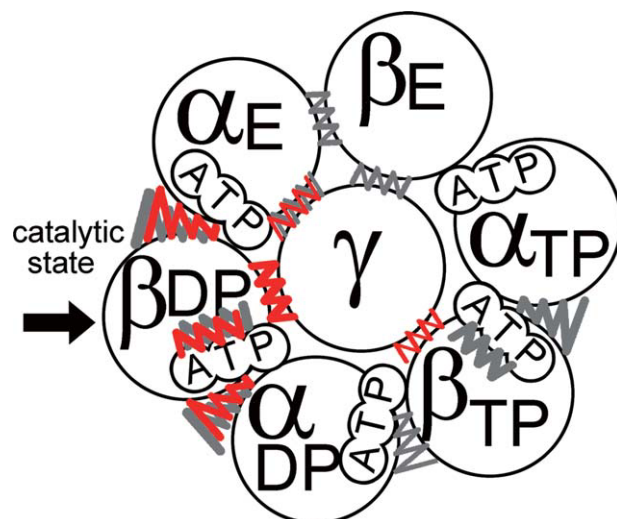


Figure 9. Summary of the concerted motions among α , β , and γ subunits and ATP. Red (gray) lines indicate concerted movements in the C-terminal (nucleotide-binding) domains. Thick (thin) lines indicate very strongly (strongly) correlated motions. The concerted motions in the N-terminal domains have been omitted, since the results show little difference for all the subunit interfaces.

β_E and β_{TP} subunits retain the same conformations as in the catalytic dwell state.²⁸ Highly correlated motions of the β_{DP} and γ subunits suggest that structural changes occurring in the β_{DP} subunit after ATP hydrolysis can effectively induce movements of the γ subunit. In addition, because the C-terminal domain of the β_{DP} subunit also moves concertedly with the adjacent α_E and α_{DP} subunits, structural changes of the β_{DP} subunit may also result in movements of the α subunits. Furthermore, since the α_E subunit also undergoes correlated motions with the γ subunit, movements of the α_E subunit may also induce γ subunit movements. Consequently, in addition to the conformational changes in the β subunits, the concerted motions arising from the various interface configurations among the subunits presumably also contribute to the γ subunit rotation.

Acknowledgments

The authors thank Prof. Shigehiko Hayashi (Kyoto University) for helpful discussions and Dr. Stephen M. Lyth (Tokyo Institute of Technology) for carefully editing the article. All computations were carried out at Tsurumi campus of Yokohama City University, Yokohama, Japan.

References

1. Futai, M.; Kanazawa, H. *Microbiol Rev* 1983, 47, 285.
2. Futai, M.; Noumi, T.; Maeda, M. *Annu Rev Biochem* 1989, 58, 111.
3. Senior, A. E. *Annu Rev Biophys Biophys Chem* 1990, 19, 7.
4. Pedersen, P. L.; Amzel, L. M. *J Biol Chem* 1993, 268, 9937.
5. Boyer, P. D. *Annu Rev Biochem* 1997, 66, 717.
6. Walker, J. E. *Angew Chem Int Ed* 1998, 37, 2308.
7. Weber, J., Sr., A. E. *Biochim Biophys Acta* 2000, 1458, 300.
8. Kinoshita, K., Jr.; Yasuda, R.; Noji, H.; Ishiwata, S.; Yoshida, M. *Cell* 1998, 93, 21.
9. Gao, Y. Q.; Yang, W.; Karplus, M. *Cell* 2005, 123, 195.
10. Karplus, M.; Gao, Y. Q. *Curr Opin Struct Biol* 2004, 14, 250.
11. Rastogi, V. K.; Girvin, M. E. *Nature* 1999, 402, 263.
12. Boyer, P. D. *Biochim Biophys Acta* 1993, 1140, 215.
13. Abrahams, J. P.; Leslie, A. G.; Lutter, R.; Walker, J. E. *Nature* 1994, 370, 621.
14. Menz, R. I.; Walker, J. E.; Leslie, A. G. *Cell* 2001, 106, 331.
15. Noji, H.; Yasuda, R.; Yoshida, M.; Kinoshita, K., Jr. *Nature* 1997, 386, 299.
16. Itoh, H.; Takahashi, A.; Adachi, K.; Noji, H.; Yasuda, R.; Yoshida, M.; Kinoshita, K., Jr. *Nature* 2004, 427, 465.
17. Yasuda, R.; Noji, H.; Kinoshita, K., Jr.; Yoshida, M. *Cell* 1998, 93, 1117.
18. Yasuda, R.; Noji, H.; Yoshida, M.; Kinoshita, K., Jr.; Itoh, H. *Nature* 2001, 410, 898.
19. Shimabukuro, K.; Yasuda, R.; Muneyuki, E.; Hara, K. Y.; Kinoshita, K., Jr.; Yoshida, M. *Proc Natl Acad Sci USA* 2003, 100, 14731.
20. Hirono-Hara, Y.; Noji, H.; Nishiura, M.; Muneyuki, E.; Hara, K. Y.; Yasuda, R.; Kinoshita, K., Jr.; Yoshida, M. *Proc Natl Acad Sci USA* 2001, 98, 13649.
21. Koga, N.; Takada, S. *Proc Natl Acad Sci USA* 2006, 103, 5367.
22. Pu, J.; Karplus, M. *Proc Natl Acad Sci USA* 2008, 105, 1192.
23. Sielaff, H.; Rennekamp, H.; Engelbrecht, S.; Junge, W. *Biophys J* 2008, 95, 4979.
24. Mao, H. Z.; Weber, J. *Proc Natl Acad Sci USA* 2007, 104, 18478.
25. Ariga, T.; Muneyuki, E.; Yoshida, M. *Nat Struct Mol Biol* 2007, 14, 841.
26. Okuno, D.; Fujisawa, R.; Iino, R.; Hirono-Hara, Y.; Imamura, H.; Noji, H. *Proc Natl Acad Sci USA* 2008, 105, 20722.
27. Sielaff, H.; Rennekamp, H.; Engelbrecht, S.; Junge, W. *Biophys J* 2008, 95, 4979.
28. Masaike, T.; Koyama-Horibe, F.; Oiwa, K.; Yoshida, M.; Nishizaka, T. *Nat Struct Mol Biol* 2008, 15, 1326.
29. Furuike, S.; Hossain, M. D.; Maki, Y.; Adachi, K.; Suzuki, T.; Kohori, A.; Itoh, H.; Yoshida, M.; Kinoshita, K., Jr. *Science* 2008, 319, 955.
30. Hossain, M. D.; Furuike, S.; Maki, Y.; Adachi, K.; Suzuki, T.; Kohori, A.; Itoh, H.; Yoshida, M.; Kinoshita, K., Jr. *Biophys J* 2008, 95, 4837.
31. Dittrich, M.; Hayashi, S.; Schulten, K. *Biophys J* 2003, 85, 2253.
32. Dittrich, M.; Hayashi, S.; Schulten, K. *Biophys J* 2004, 87, 2954.
33. Böckmann, R. A.; Grubmüller, H. *Nat Struct Biol* 2002, 9, 198.
34. Ma, J.; Flynn, T. C.; Cui, Q.; Leslie, A. G. W.; Walker, J. E.; Karplus, M. *Structure* 2002, 10, 921.
35. Antes, I.; Chandler, D.; Wang, H.; Oster, G. *Biophys J* 2003, 85, 695.
36. Cui, Q.; Li, G.; Ma, J.; Karplus, M. *J Mol Biol* 2004, 340, 345.
37. Böckmann, R. A.; Grubmüller, H. *Biophys J* 2003, 85, 1482.
38. Zheng, W. *Proteins* 2009, 76, 747.
39. Zheng, W.; Doniach, S. *Proc Natl Acad Sci USA* 2003, 100, 13253.
40. Ikeguchi, M.; Ueno, J.; Sato, M.; Kidera, A. *Phys Rev Lett* 2005, 94, 078102.
41. Bowler, M. W.; Montgomery, M. G.; Leslie, A. G. W.; Walker, J. E. *J Biol Chem* 2007, 282, 14238.
42. Sali, A.; Blundell, T. L. *J Mol Biol* 1993, 234, 779.
43. Gibbons, C.; Montgomery, M. G.; Leslie, A. G. W.; Walker, J. E. *Nat Struct Biol* 2000, 7, 1055.
44. Ikeguchi, M. *J Comput Chem* 2004, 25, 529.
45. MacKerell, A. D. Jr.; Bashford, D.; Bellott, M.; Dunbrack, R. L.; Evanseck, J. D.; Field, M. J.; Fischer, S.; Gao, J.; Guo, H.; Ha, S.; Joseph-McCarthy, D.; Kuchnir, L.; Kuczera, K.; Lau, F. T. K.; Mattos, C.; Michnick, S.; Ngo, T.; Nguyen, D. T.; Prodhom, B.; Reiher, W. E.; Roux, B.; Schlenkrich, M.; Smith, J. C.; Stote, R.; Straub, J.; Watanabe, M.; Wiorkiewicz-Kuczera, J.; Yin, D.; Karplus, M. *J Phys Chem B* 1998, 102, 3586.
46. MacKerell, A. D., Jr.; Feig, M.; Brooks, C. L., III. *J Comput Chem* 2004, 25, 1400.
47. Jorgensen, W. L.; Chandrasekhar, J.; Madura, J. D.; Impey, R. W.; Klein, M. L. *J Chem Phys* 1983, 79, 926.
48. Essmann, U.; Perera, L.; Berkowitz, M. L.; Darden, T.; Lee, H.; Pedersen, L. G. *J Chem Phys* 1995, 103, 8577.
49. McCammon, J. A.; Harvey, S. C. *Dynamics of Proteins and Nucleic Acids*; Cambridge University Press: London, 1987.
50. Oroguchi, T.; Hashimoto, H.; Shimizu, T.; Sato, M.; Ikeguchi, M. *Biophys J* 2009, 96, 2808.
51. Kagawa, R.; Montgomery, M. G.; Braig, K.; Leslie, A. G. W.; Walker, J. E. *EMBO J* 2004, 23, 2734.
52. Braig, K.; Menz, R. I.; Montgomery, M. G.; Leslie, A. G. W.; Walker, J. E. *Structure* 2000, 8, 567.
53. Yang, W.; Gao, Y. Q.; Cui, Q.; Ma, J.; Karplus, M. *Proc Natl Acad Sci USA* 2003, 100, 874.
54. Adachi, K.; Oiwa, K.; Nishizaka, T.; Furuike, S.; Noji, H.; Itoh, H.; Yoshida, M.; Kinoshita, K., Jr. *Cell* 2007, 130, 309.